AIP | Journal of Applied Physics

The role of oxygen vacancy in the photoluminescence property at room temperature of the CaTiO3

Juliana Milanez, Alberthmeiry T. de Figueiredo, Sergio de Lazaro, Valeria M. Longo, Rafael Erlo et al.

Citation: J. Appl. Phys. 106, 043526 (2009); doi: 10.1063/1.3190524
View online: http://dx.doi.org/10.1063/1.3190524
View Table of Contents: http://jap.aip.org/resource/1/JAPIAU/v106/i4
Published by the AIP Publishing LLC.

The role of oxygen vacancy in the photoluminescence property at room temperature of the $CaTiO_3$

Juliana Milanez,[1,a)] Alberthmeiry T. de Figueiredo,[2] Sergio de Lazaro,[3] Valeria M. Longo,[2] Rafael Erlo,[1] Valmor R. Mastelaro,[4] Roberto W. A. Franco,[5] Elson Longo,[2] and José A. Varela[2]

[1]*Departamento de Química, Laboratório Interdisciplinar de Eletroquímica e Cerâmica, Universidade Federal de São Carlos, P.O. Box 676, 13565-905 São Carlos, São Paulo, Brazil*

[2]*Laboratório Interdisciplinar de Eletroquímica e Cerâmica, Instituto de Química, Universidade Estadual Paulista, P.O. Box 355, 14801-970 Araraquara, São Paulo, Brazil*

[3]*Departamento de Química, Universidade Estadual de Ponta Grossa, 84030-900 Ponta Grossa, Paraná, Brazil*

[4]*Instituto de Física de São Carlos, Universidade de São Paulo, P.O. Box 369, 13560-970 São Carlos, São Paulo, Brazil*

[5]*Centro de Ciência e Tecnologia, Universidade Estadual do Norte Fluminesce, 28013-602 Campos dos Goytacazes, Rio de Janeiro, Brazil*

(Received 25 February 2009; accepted 1 July 2009; published online 31 August 2009)

In this paper, electron paramagnetic resonance, photoluminescence (PL) emission, and quantum mechanical calculations were used to observe and understand the structural order-disorder of $CaTiO_3$, paying special attention to the role of oxygen vacancy. The PL phenomenon at room temperature of $CaTiO_3$ is directly influenced by the presence of oxygen vacancies that yield structural order-disorder. These oxygen vacancies bonded at Ti and/or Ca induce new electronic states inside the band gap. Ordered and disordered $CaTiO_3$ was obtained by the polymeric precursor method. © *2009 American Institute of Physics*. [DOI: 10.1063/1.3190524]

I. INTRODUCTION

Advances in photoluminescence (PL) studies show that titanate compounds with a structural disorder present broad and intense PL at room temperature.[1–6] In particular, much work has been concentrated on $CaTiO_3$ (CT) luminescence.[7–11] These studies have shown that the broad PL emission band covering a large part of the visible spectra of the structurally disordered compounds is very similar to nanocrystalline PL emission.

The PL phenomenon at room temperature occurs due to a structural disorder of the system. However, the system cannot be fully disordered owing to a minimal order in the structure, i.e., there is an order-disorder rate, which favors the PL phenomenon in the system. PL is a powerful probe of certain short-range order aspects in the range of 2–5 Å and in a medium range 5–20 Å, e.g., clusters where the degree of local order is such that structurally inequitable sites can be distinguished because their different types of electronic transitions are linked to a specific structural arrangement.

The structural order-disorder of perovskites (especially titanates) has been followed by means of x-ray absorption near-edge spectroscopy (XANES).[12–14] XANES is one of the most suitable techniques to provide information about the atomic environment as it is unique to each element in materials. Ti *K*-edge XANES results demonstrated that before reaching complete structural order, the cationic environments had fivefold MO_5 and sixfold MO_6 coordinations (M=Ti).[11,14]

In addition, Asokan *et al.*[15] reported changes in the local environment of Ca sites in perovskite structures based on Ca *K*- and $L_{3,2}$-XANES spectra. These changes were related to electronic properties derived from those XANES spectra. Similarly, de Lazaro *et al.*[16] reported different coordination modes for calcium by Ca *K*-edge XANES results. These experimental observations suggest that PL emission is related to $[TiO_5]$ and $[CaO_{11}]$ concentrations; moreover, local structural order-disorder depends on both the modifier lattice and the former lattice.

Several authors reported structural disorder and quantum mechanics calculation[17,18] using periodic calculations DFT/B3LYP to relate the structural disorder of titanate to room temperature PL properties. The applied methodology is based on atomic displacement to study the charge transfer between $[TiO_5-TiO_6]$ clusters and electronic levels inside the band gap.

In this paper, electron paramagnetic resonance (EPR), PL emission, and quantum mechanical calculations are used to observe and understand the structural order-disorder, paying special attention to the role of oxygen vacancy. In addition, equations describing the interaction among clusters yielding PL emission in CT are proposed. The use of cluster concepts offers a simple scheme that facilitates an understanding of the effect of structural deformations on the electronic structure indeed because the most intense PL emission is evidenced in CT samples containing a certain structural order-disorder in the lattice.

II. EXPERIMENTAL

CT ordered and disordered powders were prepared by the polymeric precursor method and were kept for 20 h at

[a)]Author to whom correspondence should be addressed. FAX: +633518214. Electronic mail: jumilanez@liec.ufscar.br.

300 °C to eliminate any remaining carbon.[19] CT was then annealed at 400, 500, or 600 °C for 2 h; CT annealed at 600 °C is fully ordered. The spectral dependence of the optical absorbance for ordered (crystalline) and disordered (amorphous) materials was taken at room temperature in the total reflection mode using Cary 5*G* equipment. The PL measurements were collected using 350.7 nm exciting wavelengths of a krypton ion laser (Coherent Innova) with the nominal output power of the laser kept at 200 mW. The monochromator slit width used was 200 μm. EPR spectra were recorded on a Varian E-9 Spectrometer operating at *x*-band (9 GHz) and operating at a microwave power of 0.5 mW and modulation frequency of 100 kHz. The *g*-factor was referenced with respect to $MgO:Cr^{3+}$ ($g=1.9797$) as the external standard. Spectra were evaluated using the SIMFONIA® program. Calcium and titanium XANES spectra were collected using the D04B-XAS1 beamline. The storage ring was operated at 1.36 GeV and around 160 mA. XANES spectra were collected at the Ca and Ti *K*-edge (4205 and 4966 eV, respectively) in a transmission mode using a Si(111) channel-cut monochromator. For comparison, all spectra were background removed and normalized using as unity the first extended x-ray absorption fine structure. All experimental measurements were performed at room temperature.

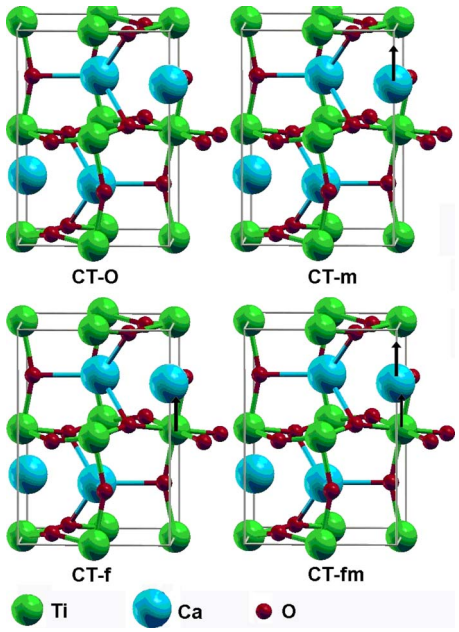

FIG. 1. (Color online) Structural models for the CT-*Pbnm* structure. (a) CT-*o*: ordered and disordered models. (b) CT-*f*: displacement of the Ti atom. (c) CT-*m*: displacement of the Ca atom. (d) CT-*fm*: simultaneous displacement of both atoms.

III. COMPUTATIONAL DETAILS

Several authors studied the PL of disordered materials at room temperature aiming to understand the behavior of electronic levels and the gap variation.[4,5,20,21] Periodic quantum mechanical calculations were made within the framework of the DFT using the Becke exchange functional,[22] combined with a gradient-corrected correlation functional by Lee, Yang and Parr, B3LYP,[23] which has been demonstrated by Muscat *et al.*[24] to be suitable for calculating structural parameters and band structures for a wide variety of solids. CT is a single phase and could be completely indexed on the basis of an orthorhombic ICDD Card No. 42-423 (*Pbnm*).[25]

The unit cell has ten atoms containing two units of $CaTiO_3$ with four nonequivalent atoms in the unit cell having internal experimental values of Ti(0.5,0,0), Ca(−0.01, 0.03, 0.25), O1(0.07,0.48,0.25), and O2(0.21,0.21,0.54). The experimental values for lattice constants *a*, *b*, and *c* are 5.37, 5.44, and 7.64 Å, respectively.

As a first step, lattice parameters were optimized to minimize the total energy with respect to the ordered system of the unit cell; Fig. 1(a) shows the CT-*o*. The calculated lattice constants were $a=5.39$ Å, $b=5.44$ Å, and $c=7.65$ Å for the ordered CT. Our theoretical lattice constant was only ~0.004% smaller than the experimental values and is in good agreement with the experimental results.

Based on the experimental XANES results presented in this paper, three theoretical models (Fig. 1) were developed to simulate the disordered types and structural complex vacancies associated with them: (i) displacement of the lattice former, Ti (CT-*f*), (ii) displacement of the lattice modifier, Ca (CT-*m*), and (iii) simultaneous displacement in the lattice former and modifier, Ti/Ca (CT-*fm*).

To represent the complex vacancies of oxygen associated with a random lattice of local units (e.g., the TiO_6 octahedral complex and CaO_{12} dodecahedral complex), it was shifted from its previous position in the unit cell for the lattice former (CT-*f* model) and lattice modifier (CT-*m* model). This displacement causes asymmetries in the unit cell; Ti is now surrounded by five oxygens in a square-based pyramidal configuration, while one other unit cell of Ti is surrounded by six oxygens as in the case of CT-*o*. Therefore, this asymmetric CT model (CT-*f*) represents the disorder in the lattice former material. This structure can be designated as $[TiO_6]-[TiO_5 \cdot V_0^z]$, where $V_0^z = V_0^x$, $V_0^{\bullet}$, and $V_0^{\bullet\bullet}$, which give rise to different complex clusters, depending on the displacement of the titanium [Fig. 1(b)].

The lattice modifier disorder (CT-*m*) was modeled by shifting the Ca from its previous position in the modifier unit cell. This displacement causes asymmetries in the unit cell where Ca is now surrounded by 11 oxygens $[CaO_{11} \cdot V_0^z]$, while Ca is surrounded by 12 oxygens $[CaO_{12}]$ as in the case of CT-*o*. Therefore, this asymmetric CT model (CT-*m*) represents the disorder in the lattice modifier material. This structure can be designated as $[CaO_{12}]-[CaO_{11} \cdot V_0^z]$, depending on the displacement of the calcium [Fig. 1(c)].

Finally, the lattice former and modifier disorder (CT-*fm*) was modeled at the same time by shifting both titanium and calcium in the same way as described above. Upon heating, three processes leading to crystallization take place in the disordered types and structural complex vacancies (cluster complex) of CT: (a) detachment of $[CaO_{11} \cdot V_0^z]$ or $[TiO_5 \cdot V_0^z]$ clusters from underbonded oxygen from their octahedral $\{[TiO_5 \cdot V_0^z]$ cluster$\}$; (a) and (b) presumably can occur simultaneously; (c) redistributing $[CaO_{11} \cdot V_0^z]$ clusters and recomposing all bonds with underbonded oxygen including those produced in (a).

All *ab initio* calculations were carried out with the CRYS-

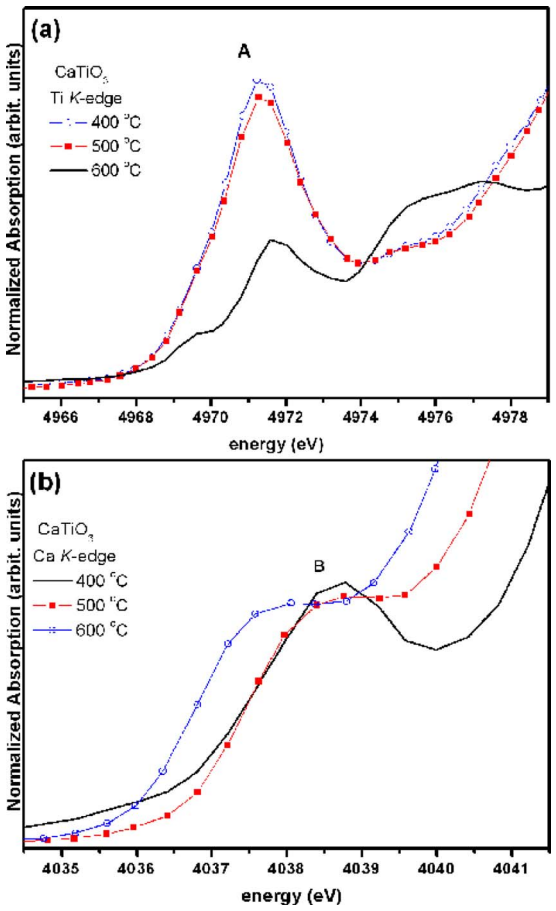

FIG. 2. (Color online) XANES spectra for CT compounds annealed at 400, 500, and 600 °C of (a) Ti *K*-edge and (b) Ca *K*-edge.

TAL98 computational code.[26] Basis set Ca, Ti, and O centers have been described in the schemes 86-511*d*3*G*, 86411-*d*(31), and 6-31*G**,[27] respectively. The Nelder–Mead algorithm[28] was used to yield theoretical lattice parameters. To simulate the displacement of the Ti and Ca atoms in the *z*-direction, the ATOMDISP option was used provided with the CRYSTAL computational code was used. For analysis of the models the results of Mulliken charges,[29] electronic levels, optical band gap, and density of states (DOS) were used.

IV. RESULTS AND DISCUSSION

Ti *K*-edge XANES spectra of CT samples as a function of the heat treatment temperature (400–600 °C) are shown in Fig. 2(a). The physical origin of the pre-edge feature *A* is the transition of the metallic 1*s* electron to an unfilled *d* state.[30] The *A* peak area was attributed to the $[TiO_5]$ concentration and therefore to PL emission.[16] Fully structurally ordered CT does not exhibit PL emission when all Ti atoms are coordinated to six oxygen atoms in a completely regular octahedron $[TiO_6]$.

The local order-disorder in the calcium site can be observed in Fig. 2(b) by a Ca *K*-edge. Based on XANES spectra,[16] the local disorder in the samples Ca *K*-edge is related to a change from the 11-fold $[CaO_{11}]$ to the 12-fold $[CaO_{12}]$ coordination number of Ca. These results of the Ca *K*-edge XANES can be related to the PL emission and the order-disorder in the calcium site, indicating that the modifier lattice can strongly affect the intensity of the PL emission due to charge exchanges between $[CaO_{11}]$ and $[CaO_{12}]$ complex clusters.

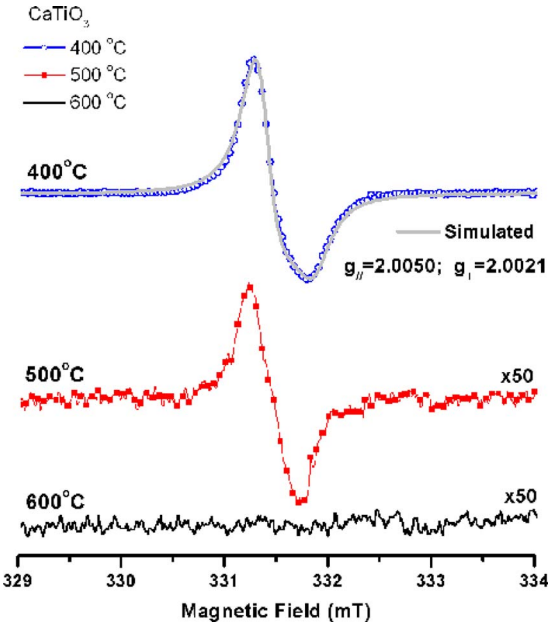

FIG. 3. (Color online) EPR spectra for CT samples annealed at 400, 500, and 600 °C.

XANES results identified the presence of several complex clusters in the disordered CT: $[TiO_6]$, $[TiO_5]$, $[CaO_{11}]$, and $[CaO_{12}]$. The existence of such complex clusters confirms the occurrence of structural defects in the material. Oxygen vacancies are important structural defects that affect the optical property of the solid. In titanates, these vacancies can occur in three different charge states: (1) the $[TiO_5 \cdot V_0^x]$ complex states have captured electrons and are neutral relative to the lattice; (2) the singly ionized $[TiO_5 \cdot V_0^{\bullet}]$ complex state; and (3) the $[TiO_5 \cdot V_0^{\bullet\bullet}]$ complex state, which did not trap any electrons and is doubly positively charged with respect to the lattice. Another portion of electrons and holes may be trapped by intrinsic crystal defects in the lattice modifier complex $[CaO_{11} \cdot V_0^z]$ complex, where $V_0^z = V_0^x$, $V_0^{\bullet}$, and $V_0^{\bullet\bullet}$. It was speculated that these oxygen vacancies induce new energy levels in the band gap and can be attributed to the calcium-oxygen or titanium-oxygen complex vacancy centers.

Direct observation of oxygen vacancies is difficult, but spectroscopic studies of doped and annealed crystals indicate the presence of these isolated vacancies.[31,32] Mestric *et al.*[33] considered the presence of six positions for an oxygen vacancy in ZrO_6. It could not be proven experimentally that only six distinct centers are involved. However, by considering the crystal structure, this observation seems to be an obvious assumption. Studies of visible luminescence in TiO_2 nanotubes and EPR spectrum show a strong signal at $g = 2.0034$,[34] which is characteristic of single-electron-trapped oxygen vacancies.[35]

CT annealed at 400 and 500 °C shows EPR signals, confirming the presence of $[TiO_5 \cdot V_0^{\bullet}]$ and/or $[CaO_{11} \cdot V_0^{\bullet}]$ species (Fig. 3). On the other hand, CT annealed at 600 °C

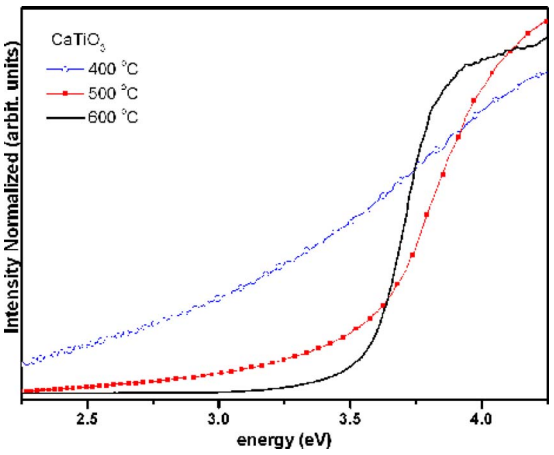

FIG. 4. (Color online) Spectral dependence of the absorbance for the CT powder samples annealed at 400, 500, and 600 °C.

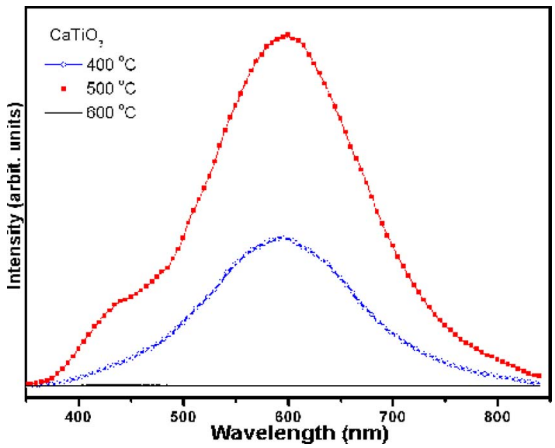

FIG. 5. (Color online) Room temperature PL spectra after exciting CT powder with a 350.7 nm laser light. CT annealed at 400, 500, and 600 °C.

does not show EPR signals, confirming the absence of $[TiO_5 \cdot V_0^{\bullet}]$ and/or $[CaO_{11} \cdot V_0^{\bullet}]$ species.

In particular, CT powder annealed at 400 °C presents a major intense feature and an asymmetric EPR line. The spin Hamiltonian parameters of the main contribution were estimated by comparison of the experimental spectrum with those generated by a computer simulation program, SINFONIA®. The calculated values of $g_{\parallel}=2.0051$ and $g_{\perp}=2.0021$ are in agreement with an axial species and are attributed to $[TiO_5 \cdot V_0^{\bullet}]$ and/or $[CaO_{11} \cdot V_0^{\bullet}]$ complex clusters in structurally disorder powders. The intensity of this line was reduced in samples annealed at 500 °C, and it vanished at 600 °C.

The presence of different complex clusters is responsible for introducing delocalized electronic levels inside the band gap acting as electron-hole pairs. These electronic levels can be confirmed by UV-vis measurements (Fig. 4), showing the spectral dependence of the absorbance for the CT samples as a function of the heat treatment temperature. Ordered materials (CT annealed at 600 °C) do not present the intermediary states inside the band gap and display an interband transition. For disordered material (CT annealed at 400 and 500 °C), this transition does not occur, but absorption edge and tails can be observed, which characterize electronic levels inside the band gap.[36–38] The optical band gaps obtained according to the Wood–Tauc method[39] (Table I) are consistent with the interpretation that the exponential optical absorption edge is controlled by the degree of structural order-disorder.[19]

TABLE I. Results of experimental and theoretical band gaps for CT.

Temperature	Band gap experimental (eV)
600 °C	3.56
500 °C	3.45
400 °C	2.60
Model	**Band gap theoretical (eV)**
Ordered	4.13
Ti 0.5z	3.55
Ca 0.5z	3.29
Ti and Ca 0.5z	3.09

Figure 5(a) shows PL spectra at room temperature, which were obtained for CT powder annealing at 400, 500, and 600 °C after excitation with a 350.7 nm laser light. The curves display a broadband distributed in the red, green, and blue regions of the visible spectrum (360–800 nm). In general, the line shape is typical of the multiphonon process, i.e., it has several relaxation channels, which are indicative of delocalized levels in the band gap. For these disordered materials, the details of band structures in solids are mainly determined by the potential within the unit cell rather than by long range periodicity. Moreover, this line shape indicates that the confinement effect cannot be considered as the predominant mechanism of the luminescence.[40] The rearrangement of the lattice was clearly detected through PL experimental measurements and is a strong indication that this measurement is highly sensitive to structural changes.

The PL spectrum for CT annealed at 500 °C is distinguished by a blue emission. Using the Gaussian method, PL spectra of the CT sample annealed at 400 and 500 °C were deconvoluted into three components: (1) the blue component (maximum below 430 nm); (2) the green component (maximum below 600 nm); and (3) the red component (maximum below 730 nm), corresponding to the regions where the maximum intensity for each component appeared. These deconvolutions represent different types of electronic transitions and are linked to a specific structural arrangement. Such electronic transitions are due to the existence of electronic levels in the band gap of a material, which are possibly due to structural disorder. Figures 5(b) and 5(c) show results obtained with such deconvolution. These graphs show that with an increase in the thermal treatment time, the red component of PL decreases and the blue component of PL increases. In the annealing process, the disorder powders become more ordered with increased annealing times; this structural change also alters the electronic levels in the band gap. The increase in blue emission is important and is attributed to delocalized electronic levels nearest the valence band (VB) and conduction band (CB).[41] With the crystallization

TABLE II. Results of Mulliken charges (q) for TiO_6, TiO_5, CaO_{12}, and CaO_{11} clusters.

	$q[TiO_6]'$	$q[TiO_5 \cdot V_0^{\bullet}]$	Δq_1	$q[CaO_{12}]'$	$q[CaO_{11} \cdot V_0^{\bullet}]$	Δq_2
Ca 0.0 and Ti 0.0	−1.55	−1.55	0	−2.18	−2.18	0
Ca 0.5z and Ti 0.0	−1.56	−1.56	0	−2.19	−1.60	−0.59
Ti 0.5z and Ca 0.0	−1.48	−0.91	−0.57	−2.10	−2.10	0
Ti 0.5z and Ca 0.5z	−1.51	−0.94	−0.57	−2.12	−1.50	−0.62

process at 600 °C, the defects vanish as well as the PL emission. The maximum intensity of the PL emission is observed for CT heat treated at 500 °C, whereas CT heat treated at 600 °C does not show PL emission, confirming that the PL intensity is associated with the thermal treatment history, structural order-disorder, and electronic levels in the band gap.[11,16]

PL results can be investigated in terms of the results of the Mulliken charge and cluster vacancies (Table II). Table II shows that the Mulliken charges for $[TiO_6]$ and $[CaO_{12}]$ complex clusters have more negative charges than $[TiO_5]$ and $[CaO_{11}]$ clusters. This quantity difference yields a charge transfer among disordered clusters to ordered clusters.[36] Therefore, the proposed displacement yields a charge transfer from the center to the surrounding area, which is similar to the order-disorder concept,[42] i.e., an effect in a localized point of the structure affects neighboring points of this structure.

Figure 6 illustrates the calculated values of VB and CB energy levels for ordered and disordered CT models and the difference between ΔE_{gap} and ΔE_{cx}. ΔE_{vx} shows the behavior of the disordered levels (displaced model) in relation to ordered levels (crystalline model) for the formation of the intermediate levels in the decay process of PL emission. In particular, this result is important because it demonstrates the formation of electronic levels with the disorder in the solid and the simultaneous presence of ordered and disordered clusters yielding crystalline defects.

The behavior of the VB and CB electronic levels directly alternates the optical band gap of the CT material. Consequently, this alteration results in the structural order-disorder. Studies on intermediate levels[5] and the order-disorder[43] showed a decrease in the optical band gap according to the structural organization. For the decrease in the optical band gap, three forms of displacement of the VB and CB can be proposed: (1) an increase in the VB energy and a decrease in the CB energy; (2) the VB energy remains constant and the CB energy decreases; and (3) an increase in the VB and CB energy remains constant. An increase in the VB energy is shown in Fig. 6, whereas the CB energy can be increased or decreased according to the displacement in the z-direction, demonstrating that the order-disorder has favorable directions for optical properties.

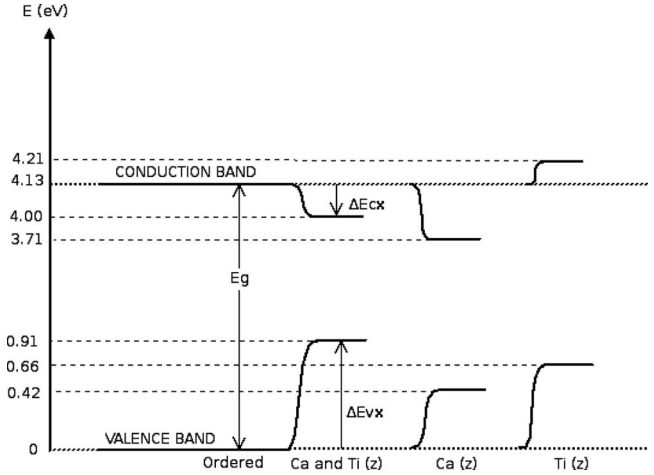

FIG. 6. Illustration of the behavior of the VB and the CB of several atomic displacements in relation to the ordered model.

Thus, it is possible to theoretically understand the influence of local disorder in the optical band gap in this oxide complex. Therefore, it can be observed in Table I that there are variations between the band gap and order-disorder due to displacements in the molecular structure of the CT material. These variations are bigger in the band gap as the displacement is localized in the z-direction, mainly Ti (z) and Ca (z). Optical properties with disorder in these directions are more interesting as they favor intermediate levels for a decay process in PL phenomena applicable to optical devices. The behavior of these electronic levels can be observed by projected DOS atomic calculated results (Fig. 7) for ordered and disordered models with Ti (z) and Ca (z). There is a main influence in the projected DOS of the O atoms in the VB, whereas the projected DOS of the cations does not have significant variations. These results show that intermediate levels or intermediate states cause a gap decrease due to the order-disorder effect of the Ca and Ti atoms according to the displacement direction.

These studies have shown that order-disordered structures in CT powders obtained by using a soft chemical synthesis are two types of coordination for titanium or calcium atoms. Oxygen vacancies in a disordered structure with $[TiO_6]'/[TiO_5 \cdot V_0^z]$ and $[CaO_{12}]'/[CaO_{11} \cdot V_0^z]$ complex clusters are electron-trapping or hole-trapping centers, according to the following equations:

$$[TiO_6]^x + [TiO_5 V_0^x] \rightarrow [TiO_6]' + [TiO_5 \cdot V_0^{\bullet}], \quad (1)$$

$$[TiO_6]^x + [TiO_5 \cdot V_0^{\bullet}] \rightarrow [TiO_6]' + [TiO_5 \cdot V_0^{\bullet\bullet}], \quad (2)$$

$$[CaO_{12}]^x + [CaO_{11} \cdot V_0^x] \rightarrow [CaO_{12}]' + [CaO_{11} \cdot V_0^{\bullet}], \quad (3)$$

$$[CaO_{12}]^x + [CaO_{11} \cdot V_0^{\bullet}] \rightarrow [CaO_{12}]' + [CaO_{11} \cdot V_0^{\bullet\bullet}], \quad (4)$$

where $[TiO_6]'$ or $[CaO_{12}]'$ are donors, $[TiO_5 \cdot V_0^{\bullet}]$ or $[CaO_{11} \cdot V_0^{\bullet}]$ are donors/acceptors $[TiO_5 \cdot V_0^{\bullet\bullet}]$, and $[CaO_{11} \cdot V_0^{\bullet\bullet}]$ are acceptors. It is assumed that charge redistribution may lead to electron-hole recombination of localized excitons.[44] This series of equations represents the complex

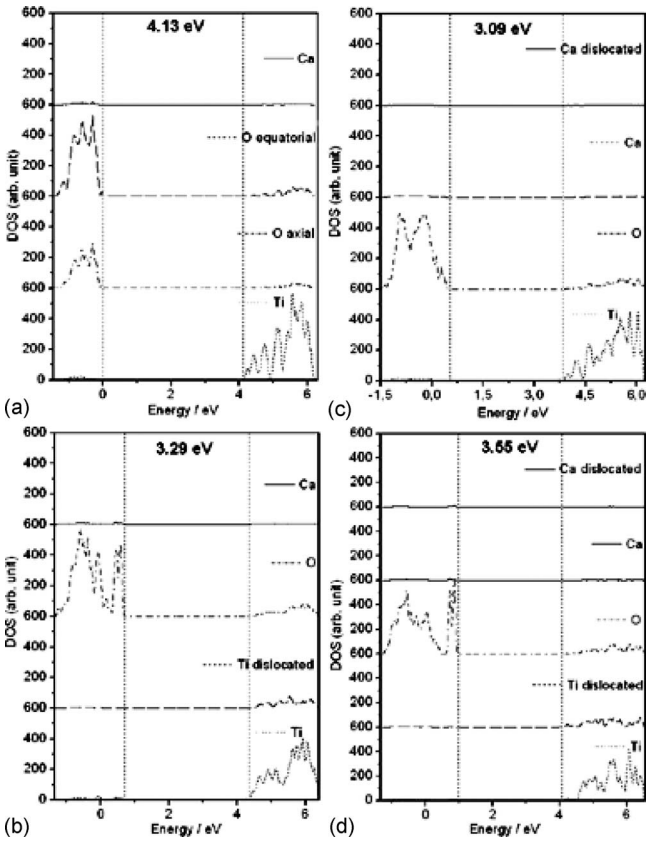

FIG. 7. Project DOS atomic levels for ordered and disordered models. (a) Ordered model. (b) Displacement of the Ti atom in the z-direction. (c) Displacement of the Ca atom in the z-direction and (d) displacement of the Ti and Ca atoms in the z-direction and the (x,y,z)-directions, respectively.

clusters in structural disordered solids and illustrates the oxygen vacancy occurrences that allow interaction between interclusters.

V. CONCLUSIONS

The PL phenomenon of the CT at room temperature is directly influenced by the presence of oxygen vacancies that yield structural order-disorder. These oxygen vacancies bonded at Ti and/or Ca induce new electronic states inside the band gap. One hole in the acceptor and one electron in the donor are yielded in the disordered CT powder.

Experimental results indicate that intermediate levels are formed in the band gap for structurally disordered CT. These intermediate levels can be provoked by the oxygen vacancies that can occur in three different charge states ($V_0^x = V_0^x$, $V_0^{\bullet}$, and $V_0^{\bullet\bullet}$). These vacancies yield $[TiO_6]$–$[TiO_5]$ and $[CaO_{12}]$–$[CaO_{11}]$ complex clusters that are responsible for PL emission at room temperature.

With these theoretical results, it is possible to propose that the atomic displacement is a reasonable approximation for modeling vacancies in the solid state. Vacancies cause structural disorder yielding charged gradient among the lattice clusters and hence leading to intermediate levels in the band gap, which is essential for PL phenomena.

ACKNOWLEDGMENTS

The authors gratefully acknowledge the financial support of the Brazilian research financing Institutions FAPESP/CEPID (Grant No. 98/14324-0), CNPq, and CAPES. The research was partially performed at LNLS-National Laboratory of Synchrotron Light, Brazil.

[1] H. Pinto and A. Stashans, Phys. Rev. B **65**, 134304 (2002).
[2] E. Heifets, R. I. Eglitis, E. A. Kotomin, J. Maier, and G. Borstel, Phys. Rev. B **64**, 235417 (2001).
[3] P. Ghosez, J. P. Michenaud, and X. Gonze, Phys. Rev. B **58**, 6224 (1998).
[4] E. Longo, E. Orhan, F. M. Pontes, C. D. Pinheiro, E. R. Leite, J. A. Varela, P. S. Pizani, T. M. Boschi, F. Lanciotti, A. Beltran, and J. Andres, Phys. Rev. B **69**, 125115 (2004).
[5] E. Orhan, J. A. Varela, A. Zenatti, M. F. C. Gurgel, F. M. Pontes, E. R. Leite, E. Longo, P. S. Pizani, A. Beltran, and J. Andres, Phys. Rev. B **71**, 085113 (2005).
[6] C. M. Liu, X. T. Zu, and W. L. Zhou, J. Phys. D: Appl. Phys. **40**, 7318 (2007).
[7] E. Pinel, P. Boutinaud, G. Bertrand, C. Caperaa, J. Cellier, and R. Mahiou, J. Alloys Compd. **374**, 202 (2004).
[8] T. Kyomen, R. Sakamoto, N. Sakamoto, S. Kunugi, and M. Itoh, Chem. Mater. **17**, 3200 (2005).
[9] X. M. Zhang, J. H. Zhang, X. Zhang, L. Chen, S. Z. Lu, and X. J. Wang, J. Lumin. **122-123**, 958 (2007).
[10] T. Wanjun and C. Donghua, J. Am. Ceram. Soc. **90**, 3156 (2007).
[11] A. T. de Figueiredo, V. M. Longo, S. de Lazaro, V. R. Mastelaro, F. S. De Vicente, A. C. Hernandes, M. S. Li, J. A. Varela, and E. Longo, J. Lumin. **126**, 403 (2007).
[12] B. Ravel and E. A. Stern, Physica B **208-209**, 316 (1995).
[13] B. Ravel, E. A. Stern, R. I. Vedrinskii, and V. Kraizman, Ferroelectrics **206**, 407 (1998).
[14] F. M. Pontes, E. Longo, E. R. Leite, E. J. H. Lee, J. A. Varela, P. S. Pizani, C. E. M. Campos, F. Lanciotti, V. Mastelaro, and C. D. Pinheiro, Mater. Chem. Phys. **77**, 598 (2003).
[15] K. Asokan, J. C. Jan, J. W. Chiou, W. F. Pong, M. H. Tsai, Y. K. Chang, Y. Y. Chen, H. H. Hsieh, H. J. Lin, Y. W. Yang, L. J. Lai, and I. N. Lin, J. Solid State Chem. **177**, 2639 (2004).
[16] S. de Lazaro, J. Milanez, A. T. de Figueiredo, V. M. Longo, V. R. Mastelaro, F. S. De Vicente, A. C. Hernandes, J. A. Varela, and E. Longo, Appl. Phys. Lett. **90**, 111904 (2007).
[17] J. R. Sambrano, E. Orhan, M. F. C. Gurgel, A. B. Campos, M. S. Goes, C. O. Paiva-Santos, J. A. Varela, and E. Longo, Chem. Phys. Lett. **402**, 491 (2005).
[18] E. Orhan, M. Anicete-Santos, M. Maurera, F. M. Pontes, C. O. Paiva-Santos, A. G. Souza, J. A. Varela, P. S. Pizani, and E. Longo, Chem. Phys. **312**, 1 (2005).
[19] F. M. Pontes, C. D. Pinheiro, E. Longo, E. R. Leite, S. R. de Lazaro, J. A. Varela, P. S. Pizani, T. M. Boschi, and F. Lanciotti, Mater. Chem. Phys. **78**, 227 (2003).
[20] E. Orhan, F. M. Pontes, C. D. Pinheiro, E. Longo, P. S. Pizani, J. A. Varela, E. R. Leite, T. M. Boschi, A. Beltran, and J. Andres, J. Eur. Ceram. Soc. **25**, 2337 (2005).
[21] S. M. Hosseini, T. Movlarooy, and A. Kompany, Physica B **391**, 316 (2007).
[22] A. D. Becke, J. Chem. Phys. **98**, 5648 (1993).
[23] C. T. Lee, W. T. Yang, and R. G. Parr, Phys. Rev. B **37**, 785 (1988).
[24] J. Muscat, A. Wander, and N. M. Harrison, Chem. Phys. Lett. **342**, 397 (2001).
[25] S. Qin, A. I. Becerro, F. Seifert, J. Gottsmann, and J. Jiang, J. Mater. Chem. **10**, 1609 (2000).
[26] V. R. Saunders, R. Dovesi, C. Roetti, M. Causa, N. M. Harrison, and C. M. Zicovich-Wilson, CRISTAL98 User's Manual, University of Torino, Torino, Italy, 1998.
[27] M. Towler, CRYSTAL98 Resources Page, 2007.
[28] J. A. Nelder and R. Mead, Comput. J. **7**, 308 (1965).
[29] R. S. Mulliken, J. Chem. Phys. **23**, 1833 (1955).
[30] R. V. Vedrinskii, V. L. Kraizman, A. A. Novakovich, P. V. Demekhin, and S. V. Urazhdin, J. Phys.: Condens. Matter **10**, 9561 (1998).
[31] R. Merkle and J. Maier, Phys. Chem. Chem. Phys. **5**, 2297 (2003).
[32] D. J. A. Gainon, J. Appl. Phys. **36**, 2325 (1965).
[33] H. Mestric, R. A. Eichel, K. P. Dinse, A. Ozarowski, J. van Tol, L. C.

Brunel, H. Kungl, M. J. Hoffmann, K. A. Schonau, M. Knapp, and H. Fuess, Phys. Rev. B **73**, 184105 (2006).
[34]L. Qian, Z. S. Jin, J. W. Zhang, Y. B. Huang, Z. J. Zhang, and Z. L. Du, Appl. Phys. A: Mater. Sci. Process. **80**, 1801 (2005).
[35]E. Serwicka, Colloids Surf. **13**, 287 (1985).
[36]E. Orhan, F. M. Pontes, M. A. Santos, E. R. Leite, A. Beltran, J. Andres, T. M. Boschi, P. S. Pizani, J. A. Varela, C. A. Taft, and E. Longo, J. Phys. Chem. B **108**, 9221 (2004).
[37]E. R. Leite, E. C. Paris, F. M. Pontes, C. A. Paskocimas, E. Longo, F. Sensato, C. D. Pinheiro, J. A. Varela, P. S. Pizani, C. E. M. Campos, and F. Lanciotti, J. Mater. Sci. **38**, 1175 (2003).
[38]P. S. Pizani, E. R. Leite, F. M. Pontes, E. C. Paris, J. H. Rangel, E. J. H. Lee, E. Longo, P. Delega, and J. A. Varela, Appl. Phys. Lett. **77**, 824 (2000).
[39]D. L. Wood and J. Tauc, Phys. Rev. B **5**, 3144 (1972).
[40]W. F. Zhang, Z. Yin, and M. S. Zhang, Appl. Phys. A: Mater. Sci. Process. **70**, 93 (2000).
[41]N. Asha Bhat, K. S. Sangunni, and K. Rao, J. Non-Cryst. Solids **319**, 192 (2003).
[42]C. Malibert, B. Dkhil, J. M. Kiat, D. Durand, J. F. Berar, and A. SpasojevicdeBire, J. Phys.: Condens. Matter **9**, 7485 (1997).
[43]R. E. Cohen, J. Phys. Chem. Solids **61**, 139 (2000).
[44]A. T. de Figueiredo, S. de Lazaro, E. Longo, E. C. Paris, J. A. Varela, M. R. Joya, and P. S. Pizani, Chem. Mater. **18**, 2904 (2006).